The Ethylmalonyl-CoA Pathway Is Used in Place of the Glyoxylate Cycle by Methylobacterium extorquens AM1 during Growth on Acetate

Kathrin Schneider, Remi Peyraud, Patrick Kiefer, Philipp Christen, Nathanael Delmotte, Stéphane Massou, Jean-Charles Portais, Julia A. Vorholt

THE JOURNAL OF BIOLOGICAL CHEMISTRY VOL. 287, NO. 1, pp. 757–766, January 2, 2012

The Ethylmalonyl-CoA Pathway Is Used in Place of the Glyoxylate Cycle by *Methylobacterium extorquens* AM1 during Growth on Acetate*[S]

Received for publication, September 16, 2011, and in revised form, November 16, 2011 Published, JBC Papers in Press, November 21, 2011, DOI 10.1074/jbc.M111.305219

Kathrin Schneider[‡], Rémi Peyraud[‡], Patrick Kiefer[‡], Philipp Christen[‡], Nathanaël Delmotte[‡], Stéphane Massou[§¶‖], Jean-Charles Portais[§¶‖], and Julia A. Vorholt[‡1]

From the [‡]Institute of Microbiology, ETH Zurich, 8093 Zurich, Switzerland, the [§]Université de Toulouse, Institut National des Sciences Appliquées, Université Paul Sabatier, Institut National Polytechnique de Toulouse, Laboratoire D'Ingénierie des Systèmes Biologiques et des Procédés, F-31077 Toulouse, France, [¶]INRA, UMR792, Ingénierie des Systèmes Biologiques et des Procédés, F-31400 Toulouse, France, and [‖]CNRS, UMR5504, F-31400 Toulouse, France

Background: The ethylmalonyl-CoA pathway represents an alternative to the glyoxylate cycle.
Results: The ethylmalonyl-CoA pathway operates during acetate growth of *Methylobacterium extorquens* and represents one of three entry points into central metabolism.
Conclusion: Isocitrate lyase-positive and -negative bacteria differ substantially in overall metabolic flux distribution.
Significance: Tight coordination must exist for operation of the citric acid cycle in conjunction with the ethylmalonyl-CoA pathway.

Acetyl-CoA assimilation was extensively studied in organisms harboring the glyoxylate cycle. In this study, we analyzed the metabolism of the facultative methylotroph *Methylobacterium extorquens* AM1, which lacks isocitrate lyase, the key enzyme in the glyoxylate cycle, during growth on acetate. MS/MS-based proteomic analysis revealed that the protein repertoire of *M. extorquens* AM1 grown on acetate is similar to that of cells grown on methanol and includes enzymes of the ethylmalonyl-CoA (EMC) pathway that were recently shown to operate during growth on methanol. Dynamic ^{13}C labeling experiments indicate the presence of distinct entry points for acetate: the EMC pathway and the TCA cycle. ^{13}C steady-state metabolic flux analysis showed that oxidation of acetyl-CoA occurs predominantly via the TCA cycle and that assimilation occurs via the EMC pathway. Furthermore, acetyl-CoA condenses with the EMC pathway product glyoxylate, resulting in malate formation. The latter, also formed by the TCA cycle, is converted to phosphoglycerate by a reaction sequence that is reversed with respect to the serine cycle. Thus, the results obtained in this study reveal the utilization of common pathways during the growth of *M. extorquens* AM1 on C1 and C2 compounds, but with a major redirection of flux within the central metabolism. Furthermore, our results indicate that the metabolic flux distribution is highly complex in this model methylotroph during growth on acetate and is fundamentally different from organisms using the glyoxylate cycle.

The ability to oxidize two-carbon compounds (C2)[2] to carbon dioxide for energy generation and assimilation of these compounds into cellular material are physiological features shared by various microorganisms. The question of how carbon assimilation is accomplished is not only important with respect to growth on C2 substrates such as acetate, but also for numerous substrates that share a common initial conversion to acetyl-CoA as the entry point into central carbon metabolism. These include abundant substrates such as fatty acids, alcohols, esters, terpenes, waxes, alkenes, and polyhydroxyalkanoates.

Oxidation of acetyl-CoA under aerobic conditions generally occurs via the TCA cycle and does not allow carbon assimilation because of decarboxylation reactions. To circumvent the steps that interfere with the net synthesis of C4 compounds from acetyl-CoA, many organisms use the glyoxylate cycle that was identified more than 50 years ago and that operates in conjunction with the TCA cycle (1, 2). Instead of being decarboxylated, the TCA cycle intermediate isocitrate is cleaved by isocitrate lyase to succinate and glyoxylate. Malate synthase, the second enzyme of the glyoxylate cycle, condenses glyoxylate and another molecule of acetyl-CoA to malate, a C4 compound.

Isocitrate lyase-negative organisms that grow on acetate but lack an operating glyoxylate cycle, including *Methylobacterium extorquens* (3), *Rhodopseudomonas* (4), *Streptomycetes* (5), and *Paracoccus* (6), must use another strategy for anaplerosis of C2 compounds. This alternative pathway has long remained a mystery (7); using biochemical studies together with mutant analysis, Erb, Alber and co-workers (8–12) discovered the EMC pathway in *Rhodobacter sphaeroides*. This pathway generates one glyoxylate and one succinyl-CoA molecule from two acetyl-CoA and two carbon dioxide molecules. Condensation of glyoxylate with acetyl-CoA produces malate. Recently, the operation of the EMC pathway during methylotrophic growth and its connection to the serine cycle in the Alphaproteobacterium *M. extorquens* AM1 was demonstrated by dynamic and steady-state ^{13}C labeling experiments (13). Under methylotrophic conditions, the EMC pathway is required to generate glyoxylate from acetyl-CoA, the carbon fixation product of the

* This work was supported by ETH Zurich Grant ETH-09 09-2.
[S] This article contains supplemental Tables S1.1–S2.5.
[1] To whom correspondence should be addressed: Institute of Microbiology, ETH Zurich, Wolfgang-Pauli-Strasse 10, 8093 Zurich, Switzerland. Tel.: 41-44-632-5524; Fax: 41-44-633-1307; E-mail: vorholt@micro.biol.ethz.ch.
[2] The abbreviations used are: C2, two carbon; C1, one carbon, EMC, ethylmalonyl-CoA; PEP, phosphoenolpyruvate; (m-)H_4F, (methylene-)tetrahydrofolate; CDW, cell dry weight; PHB, polyhydroxybutyrate.

serine cycle, to restore the acceptor molecule glyoxylate. Furthermore, it was shown that the TCA cycle is incomplete during growth on methanol because no flux through 2-oxoglutarate dehydrogenase was observed (14).

The metabolic network topology of the central carbon metabolism involved in substrate oxidation, and production of precursor metabolites during growth on acetate is well understood in isocitrate-positive organisms such as *Escherichia coli* (15–19) and *Corynebacterium glutamicum* (20, 21) but has never been studied in isocitrate lyase-negative organisms. This study is the first to provide a detailed examination of the central metabolism of an isocitrate lyase-negative organism during growth on acetate. *M. extorquens* AM1 is a well studied and biotechnologically relevant model organism with respect to its methylotrophic lifestyle (22). Here, we address three different aspects of C2 metabolism in *M. extorquens*. First, we addressed the question of how redox equivalents in the facultative methylotroph are generated during heterotrophic growth on acetate. The second goal was to identify the pathway(s) involved in acetyl-CoA assimilation and, in particular, to understand the function of the EMC pathway and its potential connection to the TCA cycle. The third aim of this study was to understand the role of the serine cycle during growth on acetate because a number of intermediates, such as serine, glycine, phosphoglycerate, and phosphoenolpyruvate (PEP), are important branching points for biomass production. In addition to methylene (m)-tetrahydrofolate (H_4F), these precursor metabolites must be synthesized from acetate. To investigate the operation of the metabolic network, with a focus on the role and function of the TCA cycle, the EMC pathway, and the serine cycle during growth of *M. extorquens* AM1 on acetate, we performed comparative proteome analysis (acetate *versus* methanol) and dynamic and steady-state ^{13}C labeling experiments.

EXPERIMENTAL PROCEDURES

Chemicals—[^{13}C]Sodium acetate (99%) was purchased from Cambridge Isotope Laboratories, and D_2O (99.8% and 99.97%) was purchased from Eurisotop. All other chemicals were purchased from Sigma.

Medium Composition and Cultivation Conditions—M. extorquens AM1 was grown on minimal medium (23) supplemented with 5 mM sodium acetate. This substrate concentration was chosen because growth was inhibited by higher acetate concentrations. A preparatory culture was grown on minimal medium plates (1.5% agar); batch cultures were inoculated with cells washed from plates with minimal medium. All of the cultures were grown in a 500-ml bioreactor (Infors-HT) with a working volume of 400 ml at 28 °C, with an aeration rate of 0.2 liters/min and stirring at 1000 rpm. The pH was kept constant at 7.0 by the addition of acetic acid (0.5 M), which allowed for substrate feeding and maintenance of the substrate concentration. The cells were harvested by centrifugation at 6000 × *g* at room temperature and frozen in liquid nitrogen until analysis.

Quantification of Acetate—Quantification of acetate was performed with a Waters Alliance 2690 HPLC and a UV-VIS detector (DAD) at 210 nm. Cell cultures were harvested with a 2-ml plastic syringe and filtered through an RC syringe filter (0.2 μm); tartaric acid was added to the cell-free supernatant as an internal standard. Organic acids were separated using a Phenomenex Rezex ROA organic acid H+ (8%, 300 × 7.8 mm) column with a flow rate of 0.5 ml/min and detected at a wavelength of 210 nm. An isocratic method was employed as described by the supplier, using 2.5 mM H_2SO_4 as the solvent. Acetate was quantified with a 0.3 mM standard deviation based on technical replicates.

Biomass Composition—The analysis of biomass composition was conducted from three biological replicates as described previously (14). Biomass yield (g of [C]/cell dry weight (CDW)/g of [C] per substrate) was calculated from the biomass production rate and the substrate uptake rate.

Proteome Analysis—Cells were resuspended in deionized water supplemented with a protease inhibitor mixture (Complete; Roche Applied Science) and passed through a small French press cell three times, followed by centrifugation (5 min, 8000 × *g*) to remove cell debris. Proteins were separated by one-dimensional SDS/PAGE (Criterion Tris-HCl gel, 10.5–14%, 13.3 × 8.7 cm; Bio-Rad) and analyzed after tryptic digestion (trypsin; Promega) by reversed phase high performance liquid chromatography coupled to high accuracy mass spectrometers as described previously (24). MS/MS spectra were searched against a data base using Mascot (Matrix Science) and X!tandem. A data base containing all annotated proteins in the *M. extorquens* AM1 genome was downloaded from the Genoscope website (25). Using a decoy data base, the false positive rate was found to be less than 0.01%. To determine significant changes in protein levels during growth on acetate compared with methanol, spectral counts of each protein were normalized to the sum of all spectra detected for each sample. Average values for each substrate were obtained from three biological replicates and were used to calculate fold changes of normalized spectral counts. To evaluate the statistical significance of observed changes, one-way analysis of variance with log2 transformation was used (26). Prior to normalization, zero values were set to one.

Dynamic Labeling Experiment—^{13}C labeling experiments were performed as described (13) with adaptations. The cells were pregrown on 5 mM acetate at natural ^{13}C abundance. Incubation of cells with labeled acetate was performed in 50-ml Falcon tubes containing 2 ml of minimal medium with 5 mM [U-^{13}C]acetate. After the addition of 1 ml of culture in exponential growth phase, the sample was continuously mixed and incubated for various times. Quenching and metabolite extraction were performed as detailed below. Calculations of ^{13}C label incorporation were conducted as described (13); the labeling fractions were normalized to the ratio of acetate with a natural ^{13}C abundance from the culture and uniformly ^{13}C-labeled acetate from fresh medium.

Sampling, Quenching, and Metabolite Extraction—For the purpose of analyzing label incorporation by mass spectrometry sampling, quenching and extraction of CoA thioesters were performed as described (13) with adaptations. Sample volumes of 3 ml containing 0.6 mg of CDW were added to 13.5 ml of −20 °C 95% acetonitrile containing 25 mM formic acid. After incubation for 10 min on ice with occasional mixing, the samples were frozen in liquid nitrogen and lyophilized. Sampling of keto acids was performed by fast filtration for salt reduction as described by Bolten *et al.* (27) with some modifications. Cell

suspensions of 3 ml (0.6 mg of CDW) were harvested by vacuum filtration and washed with 5 ml of phosphate buffer containing a 90% reduced salt concentration. Subsequently, the filter was transferred to a vessel containing boiling water as described (28) for quenching and metabolite extraction.

HPLC-MS Analysis—All of the HPLC-MS analyses were performed with a Rheos 2200 HPLC system (Flux Instruments, Basel, Switzerland) coupled to an LTQ Orbitrap mass spectrometer (Thermo Fisher Scientific, Waltham, MA) equipped with an electrospray ionization probe. CoA thioester samples were resuspended in 100 μl of ammonium formate buffer (25 mM, pH 3.5). The supernatant collected after centrifugation was analyzed by HPLC-MS as described (13) with slight modifications. For online desalting, two C_{18} analytical columns (Phenomenex, Torrance, CA) were used. The samples were loaded onto a 50 × 2.0-mm C18 column (3-μm particle size; Gemini, Phenomenex), and the sample was washed for 5 min with 100% solvent A (50 mM formic acid adjusted to pH 8.1 with NH_4OH). During desalting, the short column was connected to waste via a six-port valve, and the 100 × 2.0-mm C18 column (3-μm particle size; Gemini, Phenomenex) was equilibrated with solvent A with an additional pump. After desalting, both columns were connected in series, and the following methanol gradient was applied to separate CoA thioesters: 5 min, 5%; 15 min, 23%; 25 min, 80%; and 27 min, 80%. The HPLC-MS system was equilibrated for 6 min at initial elution conditions between two successive analyses. Keto acids were analyzed after derivatization. To this end, the samples were resuspended in 100 μl of 30 mM pentafluorobenzyl hydroxylamine as the derivatization reagent, followed by incubation for 45 min at 45 °C. Subsequently, the samples were centrifuged (4 °C, 5 min, 20,000 × *g*) and analyzed by HPLC-MS. The oximated acids were separated by reversed phase HPLC after online desalting using the same setup described above for CoA thioesters. Solvent A was 2 mM acetic acid with 4 mM NH_4OH at pH 9.3, and solvent B was methanol. A gradient was applied as follows: after 5 min of online desalting, solvent B was set linearly from 3 to 90% within 33 min. Amino acids were analyzed as described (28).

Sample Preparation and NMR Analysis—To extract proteinogenic amino acids, the cell pellets were resuspended in 20 mM Tris-HCl, pH 7.6, and disrupted by three successive freeze-thaw cycles (submersion in liquid N_2 for 10 s), three passages through a small French press cell, and three rounds of sonication (30 s at 23 kHz). Cell debris was removed by ultracentrifugation, and proteins were precipitated in 70% ethanol (final concentration) and hydrolyzed in 6 M HCl for 12 h. After deuteriation, two-dimensional [^{1}H-^{13}C]heteronuclear single quantum coherence spectroscopy and two-dimensional zero quantum filtered total correlation spectroscopy NMR spectra were recorded on a Bruker Avance II 500-MHz spectrometer as described (13, 29, 30).

Metabolic Flux Analysis—For the purpose of flux analysis, *M. extorquens* AM1 was grown in the presence of 5 mM ^{13}C-labeled acetate (80% [2-^{13}C]acetate and 20% [U-^{13}C]acetate), and the culture was aerated with synthetic air containing 5% [^{12}C]carbon dioxide. In total, three independent biological replicates were performed. The cells were inoculated at an OD_{600} of 0.01 and harvested at OD_{600} of 1. Labeling of acetate was designed to resolve fluxes in the TCA cycle, EMC pathway, serine cycle, and C1 metabolism. Flux calculations were performed using the modified reaction network (13, 14), in which the half-reaction model of the pentose-phosphate pathway (31) and phosphoacetyl transferase were introduced (see supplemental Table S2.3). Biosynthetic requirements determined from the quantification of biomass composition were included. Flux distributions were calculated from the positional and mass isotopomers of amino acids obtained by NMR and HPLC-MS (as described above) using the ^{13}C-Flux software developed by Wiechert *et al.* (32). Sensitivity analysis was conducted to establish the confidence interval of the calculated fluxes.

RESULTS

Macrokinetic Growth Characterization of M. extorquens AM1 during Growth on Acetate—M. extorquens AM1 was grown in bioreactors in the presence of acetate as its sole source of carbon and energy, whereby the growth rate decreased with increasing substrate concentration (growth rate on 5 mM acetate was 0.068 h^{-1}, compared with 0.025 h^{-1} on 30 mM acetate). The biomass yield for *M. extorquens* was 0.37 ± 0.01 g of [C]/CDW/g of [C] on 5 mM acetate. The one-dimensional ^{1}H NMR analysis of the supernatant revealed no significant accumulation of cultivation products in the medium (limit of detection: 10 μM measured at A_{600} of 1). During growth on 5 mM acetate, the specific substrate uptake rate was determined to be 4.0 ± 0.4 mmol·g^{-1} [CDW]·h^{-1}, and the proton production rate was 0.53 ± 0.05 mmol·g^{-1} [CDW]·h^{-1}. The amount of polyhydroxybutyrate (PHB) was 13 ± 0.4%, which was significantly higher than on methanol (2 ± 0.05%). The biomass composition of *M. extorquens* AM1 was determined (supplemental Tables S2.1 and S2.2) to calculate accurate biomass precursor requirements for the calculation of ^{13}C metabolic flux (see below).

Identification of Proteins Present in Cells Grown on Acetate—To determine the enzymatic framework underlying the metabolic network topology and to reveal proteins specific for growth on acetate, we performed a proteome analysis of *M. extorquens* AM1 grown on acetate. We used cultures grown in the presence of methanol as the reference because metabolism under methylotrophic conditions is well characterized (3, 13, 14, 33), as is the proteome (34, 35). Cell extracts from cells grown on acetate and methanol were loaded onto a one-dimensional SDS-PAGE and were analyzed by HPLC-MS/MS after tryptic digestion. In total, ~2600 proteins were identified (supplemental Table S1.1). Although fold changes in spectral counts are not linearly correlated with fold changes in protein amounts, this approach is suitable for determining significant variations in protein levels among different sample sets (36). To this end, fold changes in normalized spectral counts were determined, and statistical significance was tested by one-way analysis of variance. The majority of proteins detected under both growth conditions, *i.e.* acetate and methanol, did not change, thus indicating an overall consistency in the protein repertoire. Among all proteins with a p value smaller than 0.05, 53 proteins from cells grown in the presence of acetate showed a fold change higher than two relative to growth on methanol, and nine of these exhibited fold changes higher than five. Fifty-four proteins were less abundant on acetate (fold change <0.5) com-

TABLE 1

Results of proteome analysis from *M. extorquens* AM1 grown on acetate and methanol by one-dimensional SDS-PAGE followed by HPLC-MS/MS analysis

The proteins of the central metabolism are listed.

Gene number[a]	Description (gene name)	*p* value[b]	Fold change[c]
Substrate uptake and activation			
2531	Acetyl-CoA synthetase (*acs*)	<0.01	2.9
2533	Acetate transporter (*actP*)	0.12	1.7
3299	$H^{(+)}$ translocating pyrophosphatase (*hppa*)	<0.01	Only on acetate
TCA cycle			
5129	Citrate synthase (*icdB*)	<0.01	3.1
2828	Aconitate hydratase (*acnA*)	0.05	1.7
3354	$NADP^+$-dependent isocitrate dehydrogenase (*icd*)	0.01	2.4
1540, 1541, 1542	2-Oxoglutarate dehydrogenase (*sucA*, *sucB*, *lpd*)	<0.01, 0.02, 0.01	2.7, 3.6, 3.8
1538, 1539	Succinyl-CoA hydratase (*sucC*, *sucD*)	0.01, 0.07	2.0, 1.6
3860, 3861, 3863	Succinate dehydrogenase (*sdhD*, *sdhA/B*, *sdhB*)	0.05, 0.01, 0.13	2.0, 3.6, 4.1
2857	Fumarase (*fumC*)	<0.01	3.4
1537	Malate dehydrogenase (*mdh*)	0.02	1.8
C1 oxidation: H_4F/H_4MPT pathway and formate dehydrogenase			
1729	H_4F pathway: methenyl-H_4F cyclohydrolase (*fch*)	0.01	0.2
1728	H_4F pathway: methylene-H_4F dehydrogenase (*mtdA*)	<0.01	0.2
0329	H_4F pathway: formate H_4F ligase (*ftfl*)	<0.01	0.3
1766	H_4MPT pathway: formaldehyde-activating enzyme (fae)	0.01	0.6
1761	H_4MPT pathway: methylene-H_4MPT dehydrogenase (*mtdB*)	0.63	1.1
1763	H_4MPT pathway: methenyl-H_4MPT cyclohydrolase (*mch*)	0.20	0.7
1755, 1756, 1757, 1758	H_4MPT pathway: formyltransferase/hydrolase (*fhcC*, *fhcD*, *fhcA*, *fhcB*)	0.33, 0.04, 0.44, 0.07	0.8, 0.6, 0.8, 0.7
5031, 5032	NAD^+ dependent formate dehydrogenase (W-containing) (*fdh1A*, *fdh1B*)	0.01, 0.18	2.9, 1.7
4846, 4847, 4848, 4849	Formate dehydrogenase (Mo-containing), (*fdh2C*, *fdh2B*, *fhd2A*, *fdh2D*)	0.37, <0.01, <0.01, 0.12	Only on methanol
Redox balance			
2956, 2958	$NAD(P)^+$ transhydrogenase (*pntA*, *pntB*)	<0.01, 0.85	12.5, 12.3
EMC pathway			
3700	β-Ketothiolase (*phaA*)	0.08	1.6
3701	Acetoacetyl-CoA reductase (*phaB*)	0.79	1.0
3675	Crotonase (*croR*)	0.85	1.0
0178	Crotonyl-CoA carboxylase/reductase (*ccr*)	0.42	0.9
0839	Ethylmalonyl-/methylmalonyl-CoA epimerase (*epi*)	0.82	1.1
0180	Ethylmalonyl-CoA mutase (*ecm*)	0.07	0.7
2223	Methylsuccinyl-CoA dehydrogenase (*msd*)	0.56	0.9
4153	Mesaconyl-CoA hydratase (*mcd*)	0.01	0.4
1733	β-Methylmalonyl-CoA/malyl-CoA lyase (*mclA1*)	<0.01	0.2
0172, 3203	Propionyl-CoA carboxylase (*pccB*, *pccA*)	0.79, 0.06	1.1, 0.6
2390, 5251	Methylmalonyl-CoA mutase (*mcmB*, *mcmA*)	0.33, <0.01	0.8, 0.5
2137	Malyl-CoA thioesterase (*mcl2*)	0.07	1.3
PHB metabolism			
3304	PHB polymerase (*phaC*)	0.72	8.2
2218	Granule-associated 11-kDa protein	0.02	2.5
Serine cycle			
3384	Serine hydroxymethyltransferase (*glyA*)	0.03	0.7
1726	Serine-glyoxylate aminotransferase (*sga*)	<0.01	0.1
1727	Hydroxypyruvate reductase (*hpr*)	<0.01	0.2
2944	Glycerate kinase (*gck*)	<0.01	0.3
2984	Enolase (*eno*)	<0.01	1.4
1732	PEP carboxylase (*ppc*)	<0.01	0.1
1730, 1731	Malate thiokinase (*mtkA*, *mtkB*)	<0.01, <0.01	0.1, 0.1
Glycine cleavage system and phosphoserine pathway			
0620, 0622	Glycine cleavage system (*gcv*)	0.94, 0.21	34.7, 14.3
0485	Phosphoserine aminotransferase (*serC*)	0.01	0.4
2848	Phosphoserine phosphatase (*serB*)	0.35	1.3
0486	Phosphoglycerate dehydrogenase (*serA*)	0.38	0.6
C3 metabolism			
1533	PEP carboxykinase (*pckA*)	<0.01	Only on acetate
0594	Malic enzyme (*dme*)	<0.01	3.5
2941	Pyruvate kinase (*pyk*)	0.01	0.3
3097	Pyruvate phosphate dikinase (*ppdK*)	0.02	1.8
2987, 2986, 2989, 2990	Pyruvate dehydrogenase (*pdhA*, *pdhB*, *pdhC*, *lpd*)	<0.01, 0.01, <0.01, <0.01	4.5, 5.5, 8.2, 11.2

[a] Gene number (META1) reflects the order in the chromosome.
[b] Obtained from statistical analysis by one-way analysis of variance with log2 transformation.
[c] Fold change of averaged spectral counts acetate *versus* methanol.

pared with methanol, and nine of these exhibited fold changes smaller than 0.2. In total, 53 proteins were detected only in samples from cells grown on acetate, and 20 were detected only in samples from cells grown on methanol; however, most of these were of low abundance (detected with less than 0.3 ‰ of total spectral counts). All of these proteins are listed in supplemental Table S1.2; enzymes of central metabolism and their putative roles are highlighted in Table 1.

Acetate must first be activated before it can enter central metabolism. Among the proteins specifically detected or enriched during growth in the presence of acetate, an acetate transporter and acetyl-CoA synthetase were found. Because we detected higher expression of acetyl-CoA synthetase (fold change, 2.9) in cells grown on acetate compared with methanol and we could barely detect acetate kinase and phosphoacetyl-CoA transferase (both less than 0.01‰), we predict acetyl-CoA synthesis by AMP-forming acetyl-CoA synthetase. Accordingly, a proton-translocating pyrophosphate synthase was found only in acetate-grown cells; this enzyme would allow for the effective conservation of energy by coupling proton pumping across the membrane to the cleavage of pyrophosphate, the product of acetyl-CoA formation via acetyl-CoA synthetase.

All of the TCA cycle enzymes were detected during growth on acetate; all of them (with the exception of aconitate hydratase and malate dehydrogenase) exhibited a fold change greater than two relative to methanol-grown cells. The apparent increase in these proteins is consistent with the enhanced operation of the TCA cycle, which we would predict in the case of acetyl-CoA oxidation for energy generation. In principle, oxidation of C1 units to carbon dioxide could be an alternative to catabolic oxidation via the TCA cycle to generate reducing equivalents. In such a scenario, acetate could be converted to glyoxylate and subsequently to glycine, followed by decarboxylation by a glycine cleavage complex to m-H_4F, which is oxidized to formate via tetrahydrofolate (H_4F) intermediates (though this would generate NADPH rather than NADH (37)) or, indirectly, via tetrahydromethanotperin intermediates (generating NAD(P)H (38)) and subsequent oxidation of formate to carbon dioxide (39). The glycine cleavage complex was more abundant during growth on acetate, whereas it was weakly detected in methanol-grown cells. The operation of the enzyme complex can be expected to contribute to the synthesis of m-H_4F from glycine (40). Enzymes involved in one-carbon metabolism linked to H_4F and tetrahydromethanopterin (H_4MPT) were detected in acetate-grown cells. Whereas enzymes dependent on H_4MPT were present at the same order of magnitude in both acetate- and methanol-grown cells, enzymes involved in C1 unit conversion linked to H_4F were less abundant on acetate (fold change $\approx$ 0.2). Tungsten-containing NAD^+-linked formate dehydrogenase 1 (41) was more abundant (fold change $\approx$ 3) during growth on acetate than on methanol. Otherwise, pyruvate dehydrogenase could contribute to the greater degree of NADH synthesis in cells grown on acetate than on methanol (fold change $\approx$ 5–11). These alternative pathways may balance NADH/NADPH production, whereas the TCA cycle produces a fixed ratio of NADH to NADPH of 1:1. Membrane-bound $NAD(P)^+$ transhydrogenase was more abundant (fold change $\approx$ 10) in acetate-grown cells than methanol, indicating that balancing redox equivalents is critical during growth on acetate.

All of the enzymes of the EMC pathway for acetyl-CoA assimilation and conversion to glyoxylate and succinyl-CoA were detected in cells grown in the presence of acetate. Most enzymes of the EMC pathway were detected at a similar abundance during growth on acetate relative to methanol, with the exception of mesaconyl-CoA hydratase (fold change 0.4) and malyl-CoA/β-methylmalyl-CoA lyase (fold change 0.2). The latter is also part of the serine cycle, for which most proteins were less abundant during growth on acetate, suggesting a minor role for serine cycle enzymes during growth on acetate. All of the enzymes involved in the phosphoserine pathway (42) were detected in both acetate- and methanol-grown cells; only phosphoserine aminotransferase was less abundant during growth on acetate (fold change, 0.4).

The storage compound PHB was increased more than 6-fold during growth on acetate compared with methanol. Accordingly, PHB polymerase and granule-associated 11-kDa protein, which are required for PHB granule formation (43), were more abundant in cells grown on acetate.

PEP carboxykinase, which catalyzes the decarboxylation of oxaloacetate into PEP, *i.e.* operating in reverse compared with the serine cycle PEP carboxylase, was detected in acetate-grown cells. Pyruvate kinase, which is required for the conversion of PEP to pyruvate (3), was less abundant during growth on acetate than on methanol (fold change, 0.3), whereas pyruvate phosphate dikinase, which catalyzes the conversion of pyruvate to PEP (3), was more abundant (fold change, 1.8). Pyruvate may be synthesized by malic enzyme, which was more abundant during growth on acetate than on methanol (fold change, 3.5).

Dynamic Acetate Label Incorporation—A central question regarding growth on C2 substrates concerns the involvement of the EMC pathway, which converts acetyl-CoA to glyoxylate and succinyl-CoA. To demonstrate the presence of the enzymes involved (see above), as well as their operation, dynamic ^{13}C labeling experiments were performed. To this end, [U-^{13}C]acetate was mixed with a culture of cells grown on naturally labeled acetate, and ^{13}C incorporation into EMC pathway CoA thioesters was measured by HPLC-MS. In addition, incorporation of the label into the central intermediate 2-oxoglutarate was followed to monitor operation of the TCA cycle. The results are presented in Fig. 1 as percentages of ^{13}C-labeled atoms incorporated into the metabolite, normalized to the maximal number of [^{13}C]carbon atoms that can be incorporated from [U-^{13}C]acetate according to the network topology.

As expected, acetyl-CoA was the first metabolite in which the label was detected; subsequently, label incorporation into CoA thioesters of the EMC pathway was observed, in the following sequence: hydroxybutyryl-CoA, ethylmalonyl-CoA, methylsuccinyl-CoA, mesaconyl-CoA, propionyl-CoA, and methylmalonyl-CoA. After methylmalonyl-CoA, succinyl-CoA (Fig. 1*A*) was labeled, followed by 2-oxoglutarate (Fig. 1*B*). From these results, we can conclude that the EMC pathway represents an entry point for acetate. Labeling of 2-oxoglutarate was also observed, thus implicating TCA cycle activity for acetyl-CoA conversion. The slower increase in labeled succinyl-CoA relative to methylmalonyl-CoA (Fig. 1*B*) might be indicative of a complete TCA cycle and the formation of succinyl-CoA from the EMC pathway and TCA. However, exact pool sizes of intermediates or steady-state labeling experiments (see below) are required to confirm this statement.

Approximately 10 s after the addition of [^{13}C]acetate, EMC pathway intermediates reached an apparent isotopic steady state (with the exception of methylmalonyl-CoA and succinyl-CoA). Labeling did not increase further during the next 60 s

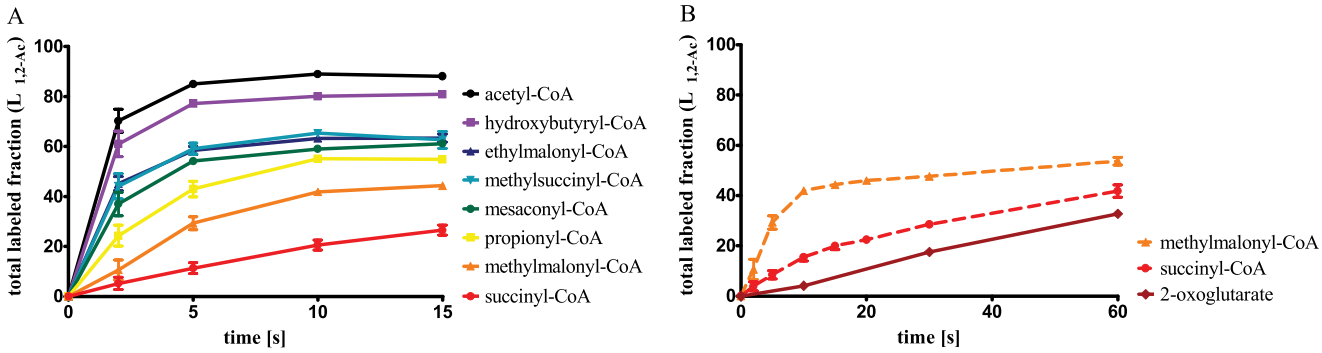

FIGURE 1. **Incorporation of the ^{13}C label in CoA thioesters (*A*) and 2-oxoglutarate (*B*) over time after incubation with [U-^{13}C]acetate.** A culture of *M. extorquens* AM1 grown on naturally labeled acetate was mixed with fresh medium containing [U-^{13}C]acetate, and label incorporation was measured in CoA thioesters and 2-oxoglutarate at different times; the average and standard deviation of three technical replicates are given in the graph. The total labeled fraction represents the percentage of ^{13}C carbon atoms that can be assimilated from [U-^{13}C]acetate. The total labeled fraction was corrected for CO_2 incorporation for intermediates of the EMC pathway (*A*).

without reaching enrichment similar to acetyl-CoA, which could be due to the recycling of PHB and/or the permanent hydrolysis and re-esterification of CoA intermediates.

Steady-state Labeling during Growth on Acetate—To quantify fluxes through the EMC pathway, the TCA cycle and more distant steps relative to the entry of acetyl-CoA, such as the operation of the serine cycle/phosphoserine pathway and the potential oxidation of glyoxylate, a ^{13}C steady-state labeling experiment and ^{13}C metabolic flux analysis were performed. Isotopomer analysis was conducted by two-dimensional heteronuclear single quantum coherence spectroscopy and two-dimensional total correlation spectroscopy NMR measurement combined with HPLC-MS using a retro-biosynthetic approach and was based on three independent biological replicates. The absolute fluxes were calculated using ^{13}C-Flux software with consideration of the acetate uptake flux and the biomass exit fluxes determined from substrate uptake, biomass composition, and growth rate. The metabolic network topology including *in vivo* flux values is presented in Fig. 2, and fluxes of the three biological replicates are provided in supplemental Table S2.4.

Flux calculations revealed that the majority of acetyl-CoA (68%) enters the TCA cycle. Notably, 98% of the acetyl-CoA entering the TCA cycle was found to be completely oxidized to CO_2; thus, the TCA cycle represents the main pathway for the generation of reducing equivalents and operates in an almost purely catabolic mode. Only 2% of acetyl-CoA entering the TCA cycle was oxidized to 2-oxoglutarate as a precursor for biomass synthesis. The second largest conversion of acetyl-CoA occurred via the EMC pathway, which converts acetyl-CoA to glyoxylate and succinyl-CoA (21%); thus, 0.8 $mmol \cdot g^{-1} \cdot h^{-1}$ of CO_2 was assimilated, which corresponds to the recycling of 16% of the completely oxidized acetate. A smaller proportion of acetyl-CoA (5%) was condensed with glyoxylate to generate malate. 3% of acetyl-CoA was used directly for biosynthesis, and 5% was used for PHB production. Oxidation of glyoxylate via glycine and m-H_4F to CO_2 could not be detected with a threshold of detection of 1%, similar to pyruvate dehydrogenase (maximum of 2%). Thus, the main pathway to generate redox equivalents upon acetate oxidation is the TCA cycle.

As mentioned above, acetyl-CoA was condensed with glyoxylate to generate malate; approximately half of the glyoxylate was converted via this route, and the remaining glyoxylate was converted to glycine by serine-glycine aminotransferase. Glycine was used for biomass synthesis (52%), cleaved by the glycine cleavage system to form m-H_4F (32%), or condensed with m-H_4F (16%) by serine hydroxymethyltransferase to generate serine. No m-H_4F was produced by serine hydroxymethyltransferase. Glycine production from glyoxylate by serine glyoxylate aminotransferase requires recycling of hydroxypyruvate, the product of serine deamination; all of the hydroxypyruvate produced was converted to 2-phosphoglycerate by serine cycle enzymes and subsequently to serine via the phosphoserine pathway. The labeling patterns of PEP and pyruvate were identical; both were derived from C4 compounds (oxaloacetate/malate). The substrate cycle of PEP carboxylase/PEP carboxykinase described during C1 assimilation (14) also exists during C2 growth and contributes to a significant loss of energy during growth on acetate (0.69 $mmol \cdot g^{-1} \cdot h^{-1}$ of ATP). No evidence for substrate cycling via malate thiokinase/malyl-CoA thioesterase was observed during growth on acetate, which is in contrast to growth in the presence of methanol.

DISCUSSION

M. extorquens AM1 can grow in the presence of acetate as its sole source of carbon and energy. To understand the catabolic and anabolic strategy of this isocitrate lyase-negative organism, proteome analysis and ^{13}C labeling experiments, including metabolic flux analysis, were conducted. The glyoxylate cycle allows for complete oxidation by the TCA cycle and replenishes metabolites that leave the cycle for biosynthetic purposes. Here, we show that the EMC pathway functionally replaces the glyoxylate cycle during growth on acetate. This recently discovered pathway operates to refill the TCA cycle; in addition, it supplies glyoxylate for glycine and serine biosynthesis. A more detailed comparison of the operation of the metabolic network revealed 20 and 30% higher rates of production of carbon dioxide and redox equivalents by isocitrate dehydrogenase and 2-oxoglutarate dehydrogenase in *M. extorquens* AM1 growing on acetate, compared with *C. glutamicum* (21) and *E. coli* (18), respectively (Table 2). This offers *M. extorquens* AM1 the addi-

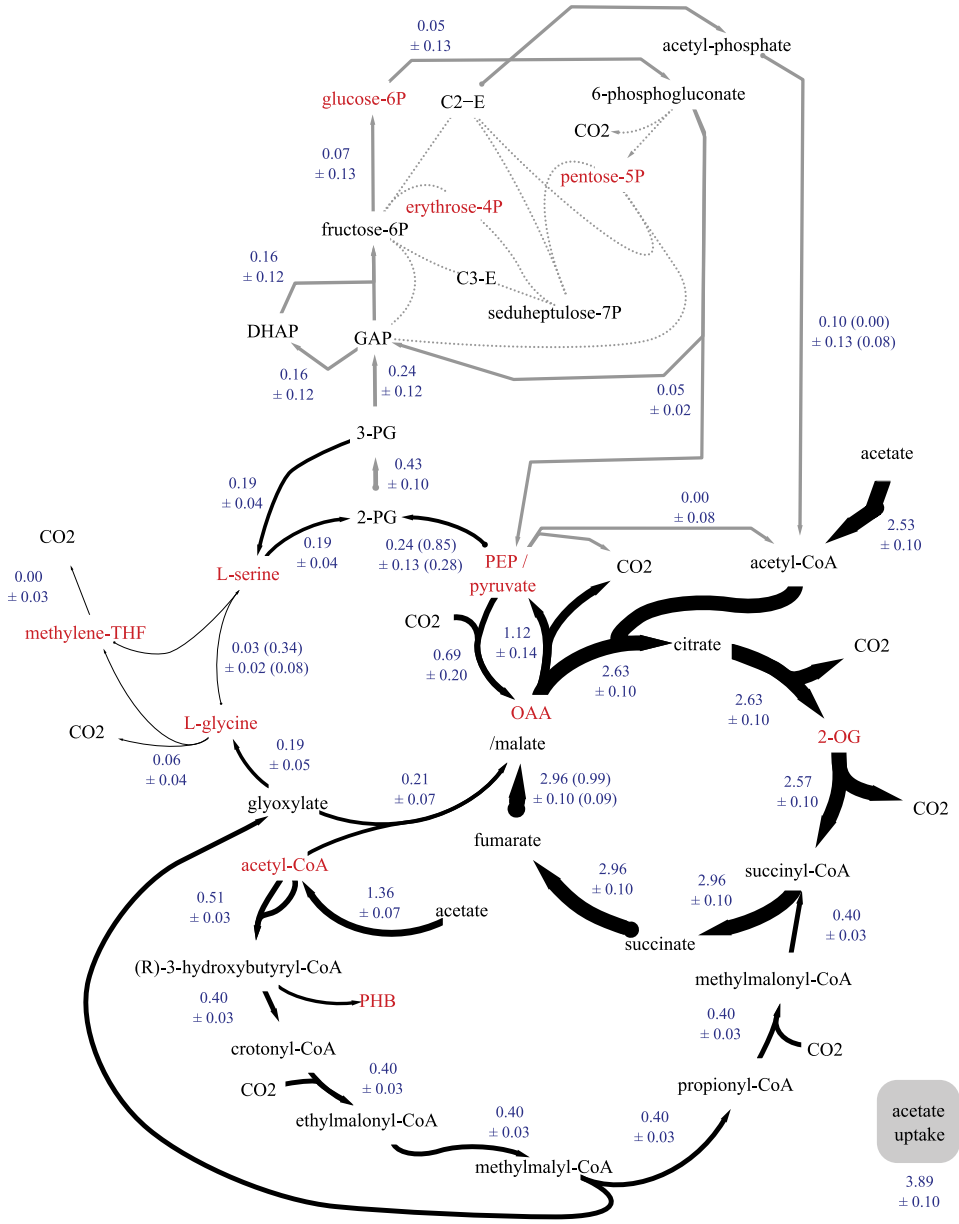

FIGURE 2. **Metabolic network topology showing the distribution of fluxes in the central metabolism of *M. extorquens* AM1 during growth on acetate.** Net fluxes obtained from ^{13}C labeling experiments are given in mmol·g^{-1} [CDW]·h^{-1}, including standard deviation; exchange fluxes are given in *parentheses*. The *arrows* represent direction of fluxes; biomass exit fluxes are labeled in *red*. The *dotted lines* indicate an unidentifiable flux. *OAA*, oxaloacetate; *2-OG*, 2-oxoglutarate; *2/3-PG*, 2/3-phosphoglycerate; *DHAP*, dihydroxyacetone-phosphate; *GAP*, glycerinaldehyd-3-phosphate; *C2-E/C3-E*, C2/C3 fragments bound to holoenzyme.

TABLE 2

Flux values relative to acetate uptake rate of (de-)carboxylating steps of TCA cycle and EMC pathway of *C. glutamicum*, *E. coli*, and *M. extorquens* AM1

The flux values were determined as indicated in the footnotes.

	C. glutamicum[a]	*E. coli*[b]	*M. extorquens* AM1[c]
Isocitrate dehydrogenase	58.1	51.0	67.6
2-Oxoglutarate dehydrogenase	56.1	49.1	66.1
Crotonyl-CoA carboxylase			10.2
Propionyl-CoA carboxylase			10.2

[a] According to Wendisch *et al.* (21).
[b] According to Zhao and Shimizu (18).
[c] According to this study.

tional gain of redox equivalents; however, these additional redox equivalents are required (by acetoacetyl-CoA reductase and crotonyl-CoA carboxylase/reductase) to operate the EMC pathway. This anaplerotic reaction sequence contains two carboxylation steps (crotonyl-CoA carboxylase and propionyl-CoA carboxylase) and recycles 20% of the carbon dioxide. The glyoxylate cycle used by *C. glutamicum* and *E. coli* neither requires redox equivalents nor contains carboxylation steps. Interestingly, despite the long and complicated reaction sequence of the EMC pathway, which operates during growth on acetate, the pathway is not disadvantageous to biomass yield.

As a consequence of the overall metabolic network topology of the EMC pathway-positive organism determined in this study, the entry points into metabolism from acetyl-CoA are clearly distinct from those in organisms with a glyoxylate cycle. For isocitrate lyase-positive organisms, two entry points for acetyl-CoA exist: the TCA cycle and malate synthase, which are stoichiometrically coupled. In the case of *M. extorquens* AM1, three independent entry points were identified in this study, in

order of their contribution: (*i*) the TCA cycle, (ii) the EMC pathway, and (iii) condensation with the EMC pathway ("side") product glyoxylate. Consequently, the network topology is more complex in the EMC pathway-positive bacterium, with the convergence of multiple pathways at different metabolites, *i.e.* succinyl-CoA fueled by the TCA cycle and the EMC pathway, and malate. As a result, fluxes must be tightly regulated to avoid metabolite imbalance at central metabolic nodes, and further investigation will be required to elucidate the underlying mechanism.

M. extorquens AM1 was the first EMC pathway-positive bacterium for which a genome scale metabolic network reconstruction was performed and for which metabolic flux analysis was accomplished under methanol growth conditions (14). The comparison performed in this study of the metabolic network under methylotrophic conditions with the network present during growth on acetate revealed a high degree of overlap in the protein repertoire. Semi-quantitative proteome analysis suggests that EMC pathway enzymes are present in quantities at the same order of magnitude or lower during growth on acetate than on methanol, which is consistent with the enzymatic activities measured by Smejkalova *et al.* (44). The latter activities were found to be higher than the flux determined via this pathway. Only the activity of ethylmalonyl-CoA mutase (0.55 mmol·g^{-1} [CDW]·h^{-1}) was in the range of the calculated flux value and could represent a growth-limiting step during acetate assimilation, which is in accordance with the earlier identification of the critical B_{12}-dependent enzyme reaction (23). However, fluxes through the EMC pathway, normalized to their respective carbon uptake rates, were identical in cells grown on methanol and acetate. Thus, it can be concluded that the EMC pathway is required for the assimilation of both substrates to the same extent relative to their carbon amount. A striking difference was observed in the operation of the TCA cycle under both conditions. The metabolic cycle operates on acetate with a high flux through 2-oxoglutarate dehydrogenase (Fig. 3), whereas it is incomplete under methylotrophic growth conditions (14). The higher flux of carbon through the catabolic TCA cycle during growth on acetate relative to the assimilatory flux in the presence of methanol is consistent with TCA cycle enzymes being more abundant on acetate than on methanol. Alternative routes for substrate oxidation during growth on acetate were determined to play only a minor role, *i.e.* the oxidation of one-carbon units and pyruvate. Thus, like nonmethylotrophic organisms, methylotrophs also use the TCA cycle as major pathway for the oxidation of acetyl-CoA.

Although a high turnover of the serine cycle is required for assimilation of one-carbon compounds to initiate the formation of multi-carbon compounds during growth on methanol, the cycle plays only a minor role during growth on acetate. This is evident from the observation that most enzymes were less abundant during growth on acetate and is consistent with the results from the flux analysis (Fig. 3). However, in the case of serine hydroxymethyltransferase, only a minor fold change in normalized spectral counts was observed (≈1.5), but flux decreased ~70-fold. The integration of data obtained from the flux analysis and proteomics suggests a post-translational flux control of serine hydroxymethyltransferase, for example, by

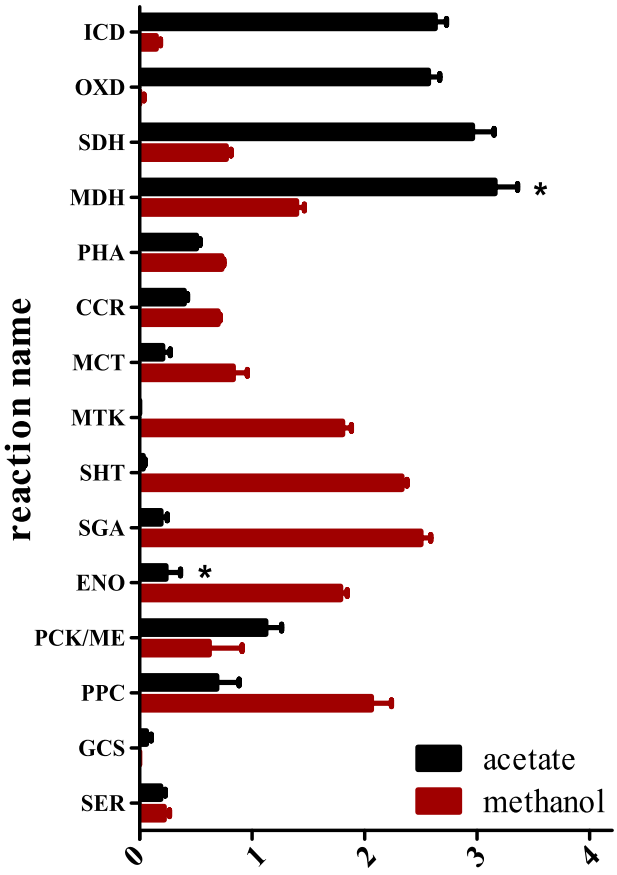

FIGURE 3. **Comparison of the flux distribution in *M. extorquens* AM1 grown on acetate and methanol.** Flux values are given in mmol·g^{-1} [CDW]·g^{-1}, and an *asterisk* indicates reversed flux on acetate relative to methanol. *ICD*, isocitrate dehydrogenase; *OXD*, 2-oxoglutarate dehydrogenase; *SDH*, succinate dehydrogenase; *MDH*, malate dehydrogenase; *PHA*, β-ketothiolase; *CCR*, crotonyl-CoA carboxylase/reductase; *MCT*, malyl-CoA thioesterase; *MTK*, malate thiokinase; *SHT*, serine hydroxymethyltransferase; *SGA*, serine glyoxylate aminotransferase; *ENO*, enolase; *PCK/ME*, PEP carboxykinase plus malic enzyme; *PPC*, PEP carboxylase; *GCS*, glycine cleavage system; *SER*, phosphoserine aminotransferase.

substrate concentrations below the K_m value or by allosteric/competitive enzyme inhibition. Not only was the flux through the serine cycle significantly lower on acetate, but also, at some steps, the net flux direction changed, resulting in a bidirectional operation of the serine "cycle" relative to its classical operation under methylotrophic growth conditions. The flux from glyoxylate to 2-phosphoglycerate via glycine and serine operated in the same direction during growth on acetate and methanol. However, the subsequent steps of the serine cycle, the conversion of 2-phosphogycerate to malate and its subsequent cleavage to glyoxylate and acetyl-CoA, exhibited a reversed flux direction during growth on acetate, despite the irreversible enzymatic reactions catalyzed by PEP carboxylase and malate thiokinase. This is achieved by their substitution with PEP carboxykinase and malyl-CoA thioesterase, respectively. Consequently, all C3 compounds (PEP, pyruvate, and phosphoglycerate) are synthesized by decarboxylation of the C4 intermediates malate and oxaloacetate. However, glycine and serine are synthesized from glyoxylate.

Integrating proteome data and ^{13}C metabolic flux analysis allowed us to correlate the abundance of proteins and their *in*

vivo activities in *M. extorquens* AM1 during growth on acetate. A high degree of overlap in the proteome between acetate- and methanol-grown cells was identified, but the connectivity of the metabolic network changed, and fluxes were redirected. This feature should allow the organism to quickly adapt to changes in carbon source availability.

REFERENCES

1. Kornberg, H. L., and Krebs, H. A. (1957) Synthesis of cell constituents from C2-units by a modified tricarboxylic acid cycle. *Nature* **179,** 988–991
2. Kornberg, H. L., and Madsen, N. B. (1957) Synthesis of C4-dicarboxylic acids from acetate by a glyoxylate bypass of the tricarboxylic acid cycle. *Biochim. Biophys. Acta* **24,** 651–653
3. Anthony, C. (1982) *The Biochemistry of Methylotrophs*, Academic Press, London
4. Albers, H., and Gottschalk, G. (1976) Acetate metabolism in *Rhodopseudomonas gelatinosa* and several other Rhodospirillaceae. *Arch. Microbiol.* **111,** 45–49
5. Han, L., and Reynolds, K. A. (1997) A novel alternate anaplerotic pathway to the glyoxylate cycle in streptomycetes. *J. Bacteriol.* **179,** 5157–5164
6. Gottschal, J. C., and Kuenen, J. G. (1980) Mixotrophic growth of *Thiobacillus*-A2 on acetate and thiosulfate as growth limiting substrates in the chemostat. *Arch. Microbiol.* **126,** 33–42
7. Anthony, C. (2011) How half a century of research was required to understand bacterial growth on C1 and C2 compounds: the story of the serine cycle and the ethylmalonyl-CoA pathway. *Sci. Prog.* **94,** 109–137
8. Erb, T. J., Berg, I. A., Brecht, V., Müller, M., Fuchs, G., and Alber, B. E. (2007) Synthesis of C5-dicarboxylic acids from C2-units involving crotonyl-CoA carboxylase/reductase: the ethylmalonyl-CoA pathway. *Proc. Natl. Acad. Sci. U.S.A.* **104,** 10631–10636
9. Erb, T. J., Brecht, V., Fuchs, G., Müller, M., and Alber, B. E. (2009) Carboxylation mechanism and stereochemistry of crotonyl-CoA carboxylase/reductase, a carboxylating enoyl-thioester reductase. *Proc. Natl. Acad. Sci. U.S.A.* **106,** 8871–8876
10. Erb, T. J., Frerichs-Revermann, L., Fuchs, G., and Alber, B. E. (2010) The apparent malate synthase activity of *Rhodobacter sphaeroides* is due to two paralogous enzymes, (3S)-malyl-coenzyme A (CoA)/{beta}-methylmalyl-CoA lyase and (3S)-malyl-CoA thioesterase. *J. Bacteriol.* **192,** 1249–1258
11. Erb, T. J., Fuchs, G., and Alber, B. E. (2009) (2S)-Methylsuccinyl-CoA dehydrogenase closes the ethylmalonyl-CoA pathway for acetyl-CoA assimilation. *Mol. Microbiol.* **73,** 992–1008
12. Alber, B. E., Spanheimer, R., Ebenau-Jehle, C., and Fuchs, G. (2006) Study of an alternate glyoxylate cycle for acetate assimilation by *Rhodobacter sphaeroides*. *Mol. Microbiol.* **61,** 297–309
13. Peyraud, R., Kiefer, P., Christen, P., Massou, S., Portais, J. C., and Vorholt, J. A. (2009) Demonstration of the ethylmalonyl-CoA pathway by using 13C metabolomics. *Proc. Natl. Acad. Sci. U.S.A.* **106,** 4846–4851
14. Peyraud, R., Schneider, K., Kiefer, P., Massou, S., Vorholt, J. A., and Portais, J. C. (2011) Genome-scale reconstruction and system level investigation of the metabolic network of *Methylobacterium extorquens* AM1. *BMC Syst. Biol.* **5,** 189
15. Holms, H. (1996) Flux analysis and control of the central metabolic pathways in *Escherichia coli*. *FEMS Microbiol. Rev.* **19,** 85–116
16. Oh, M. K., Rohlin, L., Kao, K. C., and Liao, J. C. (2002) Global expression profiling of acetate-grown *Escherichia coli*. *J. Biol. Chem.* **277,** 13175–13183
17. Walsh, K., and Koshland, D. E., Jr. (1984) Determination of flux through the branch point of two metabolic cycles: the tricarboxylic acid cycle and the glyoxylate shunt. *J. Biol. Chem.* **259,** 9646–9654
18. Zhao, J., and Shimizu, K. (2003) Metabolic flux analysis of *Escherichia coli* K12 grown on 13C-labeled acetate and glucose using GC-MS and powerful flux calculation method. *J. Biotechnol.* **101,** 101–117
19. Peng, L., and Shimizu, K. (2003) Global metabolic regulation analysis for *Escherichia coli* K12 based on protein expression by 2-dimensional electrophoresis and enzyme activity measurement. *Appl. Microbiol. Biotechnol.* **61,** 163–178
20. Gerstmeir, R., Wendisch, V. F., Schnicke, S., Ruan, H., Farwick, M., Reinscheid, D., and Eikmanns, B. J. (2003) Acetate metabolism and its regulation in *Corynebacterium glutamicum*. *J. Biotechnol.* **104,** 99–122
21. Wendisch, V. F., de Graaf, A. A., Sahm, H., and Eikmanns, B. J. (2000) Quantitative determination of metabolic fluxes during coutilization of two carbon sources: comparative analyses with *Corynebacterium glutamicum* during growth on acetate and/or glucose. *J. Bacteriol.* **182,** 3088–3096
22. Schrader, J., Schilling, M., Holtmann, D., Sell, D., Filho, M. V., Marx, A., and Vorholt, J. A. (2009) Methanol-based industrial biotechnology: current status and future perspectives of methylotrophic bacteria. *Trends Biotechnol.* **27,** 107–115
23. Kiefer, P., Buchhaupt, M., Christen, P., Kaup, B., Schrader, J., and Vorholt, J. A. (2009) Metabolite profiling uncovers plasmid-induced cobalt limitation under methylotrophic growth conditions. *PLoS One* **4,** e7831
24. Delmotte, N., Knief, C., Chaffron, S., Innerebner, G., Roschitzki, B., Schlapbach, R., von Mering, C., and Vorholt, J. A. (2009) Community proteogenomics reveals insights into the physiology of phyllosphere bacteria. *Proc. Natl. Acad. Sci. U.S.A.* **106,** 16428–16433
25. Vuilleumier, S., Chistoserdova, L., Lee, M. C., Bringel, F., Lajus, A., Zhou, Y., Gourion, B., Barbe, V., Chang, J., Cruveiller, S., Dossat, C., Gillett, W., Gruffaz, C., Haugen, E., Hourcade, E., Levy, R., Mangenot, S., Muller, E., Nadalig, T., Pagni, M., Penny, C., Peyraud, R., Robinson, D. G., Roche, D., Rouy, Z., Saenampechek, C., Salvignol, G., Vallenet, D., Wu, Z., Marx, C. J., Vorholt, J. A., Olson, M. V., Kaul, R., Weissenbach, J., Médigue, C., and Lidstrom, M. E. (2009) *Methylobacterium* genome sequences: a reference blueprint to investigate microbial metabolism of C1 compounds from natural and industrial sources. *PLoS One* **4,** e5584
26. Pham, T. V., Piersma, S. R., Warmoes, M., and Jimenez, C. R. (2010) On the beta-binomial model for analysis of spectral count data in label-free tandem mass spectrometry-based proteomics. *Bioinformatics* **26,** 363–369
27. Bolten, C. J., Kiefer, P., Letisse, F., Portais, J. C., and Wittmann, C. (2007) Sampling for metabolome analysis of microorganisms. *Anal. Chem.* **79,** 3843–3849
28. Kiefer, P., Portais, J. C., and Vorholt, J. A. (2008) Quantitative metabolome analysis using liquid chromatography-high-resolution mass spectrometry. *Anal. Biochem.* **382,** 94–100
29. Massou, S., Nicolas, C., Letisse, F., and Portais, J. C. (2007) NMR-based fluxomics: quantitative 2D NMR methods for isotopomers analysis. *Phytochemistry* **68,** 2330–2340
30. Massou, S., Nicolas, C., Letisse, F., and Portais, J. C. (2007) Application of 2D-TOCSY NMR to the measurement of specific 13C-enrichments in complex mixtures of 13C-labeled metabolites. *Metab. Eng.* **9,** 252–257
31. Kleijn, R. J., van Winden, W. A., van Gulik, W. M., and Heijnen, J. J. (2005) Revisiting the 13C-label distribution of the non-oxidative branch of the pentose phosphate pathway based upon kinetic and genetic evidence. *FEBS J.* **272,** 4970–4982
32. Wiechert, W., Möllney, M., Petersen, S., and de Graaf, A. A. (2001) A universal framework for 13C metabolic flux analysis. *Metab. Eng.* **3,** 265–283
33. Chistoserdova, L., Chen, S. W., Lapidus, A., and Lidstrom, M. E. (2003) Methylotrophy in *Methylobacterium extorquens* AM1 from a genomic point of view. *J. Bacteriol.* **185,** 2980–2987
34. Laukel, M., Rossignol, M., Borderies, G., Völker, U., and Vorholt, J. A. (2004) Comparison of the proteome of *Methylobacterium extorquens* AM1 grown under methylotrophic and nonmethylotrophic conditions. *Proteomics* **4,** 1247–1264
35. Bosch, G., Skovran, E., Xia, Q., Wang, T., Taub, F., Miller, J. A., Lidstrom, M. E., and Hackett, M. (2008) Comprehensive proteomics of *Methylobacterium extorquens* AM1 metabolism under single carbon and nonmethylotrophic conditions. *Proteomics* **8,** 3494–3505
36. Bantscheff, M., Schirle, M., Sweetman, G., Rick, J., and Kuster, B. (2007) Quantitative mass spectrometry in proteomics: a critical review. *Anal. Bioanal. Chem.* **389,** 1017–1031
37. Vorholt, J. A., Chistoserdova, L., Lidstrom, M. E., and Thauer, R. K. (1998) The NADP-dependent methylene tetrahydromethanopterin dehydrogenase in *Methylobacterium extorquens* AM1. *J. Bacteriol.* **180,** 5351–5356

38. Hagemeier, C. H., Chistoserdova, L., Lidstrom, M. E., Thauer, R. K., and Vorholt, J. A. (2000) Characterization of a second methylene tetrahydromethanopterin dehydrogenase from *Methylobacterium extorquens* AM1. *Eur. J. Biochem.* **267,** 3762–3769
39. Chistoserdova, L., Laukel, M., Portais, J. C., Vorholt, J. A., and Lidstrom, M. E. (2004) Multiple formate dehydrogenase enzymes in the facultative methylotroph *Methylobacterium extorquens* AM1 are dispensable for growth on methanol. *J. Bacteriol.* **186,** 22–28
40. Okubo, Y., Yang, S., Chistoserdova, L., and Lidstrom, M. E. (2010) Alternative route for glyoxylate consumption during growth on two-carbon compounds by *Methylobacterium extorquens* AM1. *J. Bacteriol.* **192,** 1813–1823
41. Laukel, M., Chistoserdova, L., Lidstrom, M. E., and Vorholt, J. A. (2003) The tungsten-containing formate dehydrogenase from *Methylobacterium extorquens* AM1: purification and properties. *Eur. J. Biochem.* **270,** 325–333
42. Harder, W., and Quayle, J. R. (1971) The biosynthesis of serine and glycine in Pseudomonas AM1 with special reference to growth on carbon sources other than C1 compounds. *Biochem. J.* **121,** 753–762
43. Korotkova, N., Chistoserdova, L., and Lidstrom, M. E. (2002) Poly-beta-hydroxybutyrate biosynthesis in the facultative methylotroph *Methylobacterium extorquens* AM1: identification and mutation of gap11, gap20, and phaR. *J. Bacteriol.* **184,** 6174–6181
44. Smejkalova, H., Erb, T. J., and Fuchs, G. (2010) Methanol assimilation in *Methylobacterium extorquens* AM1: Demonstration of all enzymes and their regulation. *PLoS One* **5,** e13001

The Ethylmalonyl-CoA Pathway Is Used in Place of the Glyoxylate Cycle by *Methylobacterium extorquens* AM1 during Growth on Acetate

Kathrin Schneider, Rémi Peyraud, Patrick Kiefer, Philipp Christen, Nathanaël Delmotte, Stéphane Massou, Jean-Charles Portais and Julia A. Vorholt

J. Biol. Chem. 2012, 287:757-766.
doi: 10.1074/jbc.M111.305219 originally published online November 21, 2011